Int. J. Solids Structures Vol. 26, No. 7, pp. 801–811, 1990
Printed in Great Britain.

0020–7683/90 $3.00 + .00

PARAMETRIC INSTABILITY OF LAMINATED COMPOSITE PLATES WITH TRANSVERSE SHEAR DEFORMATION

J. MOORTHY and J. N. REDDY
Department of Engineering Science and Mechanics, Virginia Polytechnic Institute and State University, Blacksburg, VA 24061, U.S.A.

and

R. H. PLAUT
Charles E. Via, Jr, Department of Civil Engineering, Virginia Polytechnic Institute and State University, Blacksburg, VA 24061, U.S.A.

(*Received* 25 *July* 1989; *in revised form* 28 *September* 1989)

Abstract—The instability of composite laminated plates under uniaxial, harmonically-varying, in-plane loads is investigated. Both symmetric cross-ply laminates and antisymmetric angle-ply laminates are analyzed. The first-order shear deformation plate theory is used to model composite laminates. The resulting linear equations of motion are transformed into small, uncoupled sets of equations, and instability regions in the plane of load amplitude versus load frequency are determined using the finite element method. The effects of damping, ratio of edge length to thickness of the plate, orthotropy, boundary conditions, number of layers and lamination angles on instability regions are examined.

1. INTRODUCTION

The instability of rectangular, composite, laminated plates subjected to harmonically-varying, in-plane loads has been investigated in several papers. Birman (1985) considered unsymmetrically laminated cross-ply plates under biaxial loading. The edges were assumed to be simply supported so that closed-form solutions exist for the vibration modes, and the modal amplitudes are governed by uncoupled Mathieu equations. Damping was neglected, and the principal instability region was determined. In addition, plates with large aspect ratios were treated for both symmetric and unsymmetric laminations.

Srinivasan and Chellapandi (1986) analyzed laminated plates under uniaxial loading. The edges were clamped and the finite strip method was used to discretize the problem. With damping neglected, a set of coupled Mathieu equations was obtained, and Hill's method of infinite determinants was applied to obtain instability regions. The effects of the aspect ratio, static in-plane load, and lamination scheme (symmetric, antisymmetric or asymmetric) on the principal instability region were examined.

Transverse shear deformation often has an important influence on the behavior of laminated plates (Reddy, 1984). Bert and Birman (1987) used a first-order shear deformation theory in an analysis of the parametric instability of unsymmetric angle-ply plates. The edges were simply supported with no in-plane displacements perpendicular to the edge and no tangential stress. As in Birman (1985), this allowed for a closed-form solution and led to uncoupled Mathieu equations (with damping neglected). For uniaxial loading, principal instability regions were determined and the effects of the aspect ratio, thickness-to-edge length ratio, number of layers, and magnitudes of the shear correction coefficients were studied.

Some related work also should be mentioned. Birman and Bert (1988) used nonlinear equations of motion and determined frequency–amplitude relationships for antisymmetrically laminated angle-ply plates under harmonic in-plane loads. Birman and Zahed (1989) investigated the response of such plates when they are not initially flat. Bert and Birman (1988) analyzed the parametric instability of orthotropic, circular cylindrical shells using a first-order shear deformation theory. Finally, Birman (1989) treated laminated plates subjected to in-plane loads which were applied suddenly (step loads) or increased

linearly with time, and Tylikowski (1989) examined dynamic stability under random in-plane loads.

In the present paper, the finite element method is used to study parametric instability of composite laminated plates. This allows various complexities, such as different sets of boundary conditions and geometries, to be considered. It is assumed that transverse shear deformations are not negligible, and a first-order shear deformation theory is applied. Symmetric cross-ply laminates and antisymmetric angle-ply laminates are analyzed.

Square plates are considered, with three sets of boundary conditions. The load is uniaxial and does not have a static component. Several solution methods are used: two approximations based on Bolotin's method; an approximation in which weak coupling between equations is neglected; and numerical integration of the equations of motion. The principal instability region is computed, as well as other regions for one case. The effects of damping, ratio of edge length to thickness of the plate, orthotropy, boundary conditions, number of layers and lamination angles are investigated.

2. GOVERNING EQUATIONS

The plate, shown in Fig. 1, has edge lengths a, thickness h, and density ρ, and is subjected to a uniformly distributed, normal in-plane load $N\cos\omega t$ along the edges $x = 0, a$. The first-order shear deformation theory involves shear correction coefficients k_4, k_5 (Hildebrand *et al.*, 1949; Mindlin, 1951; Noor and Burton, 1989). A linear strain–displacement relationship is assumed. The constitutive relations are based on the plane-stress assumption for each ply, and the lamina stiffnesses are restricted to those for an orthotropic lamina.

The mid-plane displacements along the x, y and z axes are denoted u, v and w, respectively, and the bending slopes in the xz and yz planes are ψ_x and ψ_y, respectively. The extensional, coupling and bending stiffnesses are given by (Reddy, 1984; Jones, 1975):

$$A_{ij} = \sum_{k=1}^{n} Q_{ij}^{(k)}(z_{k+1} - z_k),$$

$$B_{ij} = \sum_{k=1}^{n} Q_{ij}^{(k)}(z_{k+1}^2 - z_k^2)/2,$$

$$D_{ij} = \sum_{k=1}^{n} Q_{ij}^{(k)}(z_{k+1}^3 - z_k^3)/3, \tag{1}$$

respectively, where k denotes a typical ply, n is the total number of plies, z_k is the z coordinate of the bottom of the kth ply, and $Q_{ij}^{(k)}$ are the transformed, plane stress-reduced elastic stiffnesses.

The constitutive relations for the in-plane stress resultants N_i and stress couples M_i are given (in general form) by (Jones, 1975):

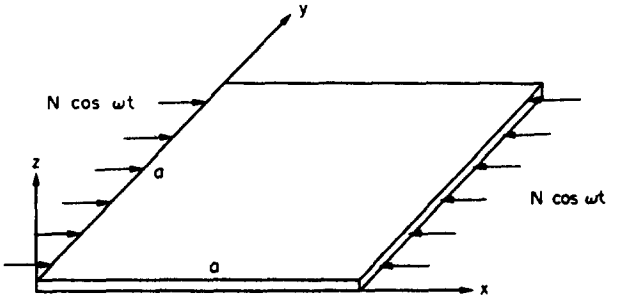

Fig. 1. Geometry of plate.

$$\begin{Bmatrix} N_1 \\ N_2 \\ N_6 \\ M_1 \\ M_2 \\ M_6 \end{Bmatrix} = \begin{bmatrix} A_{11} & A_{12} & A_{16} & B_{11} & B_{12} & B_{16} \\ A_{12} & A_{22} & A_{26} & B_{12} & B_{22} & B_{26} \\ A_{16} & A_{26} & A_{66} & B_{16} & B_{26} & B_{66} \\ B_{11} & B_{12} & B_{16} & D_{11} & D_{12} & D_{16} \\ B_{12} & B_{22} & B_{26} & D_{12} & D_{22} & D_{26} \\ B_{16} & B_{26} & B_{66} & D_{16} & D_{26} & D_{66} \end{bmatrix} \begin{Bmatrix} u_{,x} \\ v_{,y} \\ v_{,x}+u_{,y} \\ \psi_{x,x} \\ \psi_{y,y} \\ \psi_{y,x}+\psi_{x,y} \end{Bmatrix} \tag{2}$$

and those for the shear stress resultants Q_i are

$$\begin{Bmatrix} Q_2 \\ Q_1 \end{Bmatrix} = \begin{bmatrix} k_4^2 A_{44} & k_4 k_5 A_{45} \\ k_4 k_5 A_{45} & k_5^2 A_{55} \end{bmatrix} \begin{Bmatrix} w_{,y}+\psi_y \\ w_{,x}+\psi_x \end{Bmatrix} \tag{3}$$

where subscripts following commas denote partial derivatives. For symmetric cross-ply laminates, A_{16}, A_{26}, all B_{ij}, D_{16} and D_{26} are zero. For antisymmetric angle-ply laminates, A_{16}, A_{26}, B_{11}, B_{12}, B_{22}, D_{16} and D_{26} are zero.

Finally, the equations of motion are

$$\begin{aligned} N_{1,x}+N_{6,y} &= \rho h u_{,tt} \\ N_{6,x}+N_{2,y} &= \rho h v_{,tt} \\ Q_{1,x}+Q_{2,y}-(N\cos\omega t)w_{,xx} &= \rho h w_{,tt} \\ M_{1,x}+M_{6,y}-Q_1 &= (\rho h^3/12)\psi_{x,tt} \\ M_{6,x}+M_{2,y}-Q_2 &= (\rho h^3/12)\psi_{y,tt} \end{aligned} \tag{4}$$

where ρ denotes density of the material.

For the finite element model, the plate is divided into two-dimensional, rectangular, four-node, bilinear elements. Numerical integration over each element is carried out using Gauss–Legendre quadrature (Reddy, 1984). The equations of motion (4) then take the matrix form

$$[M]\{\ddot{\Delta}\}+[C]\{\dot{\Delta}\}+[K]\{\Delta\}+N\cos\omega t[S]\{\Delta\} = 0 \tag{5}$$

where $\{\Delta\}$ is the vector containing the nodal values of the generalized displacements, $[M]$ is the global mass matrix, $[C]$ is a damping matrix which has been added to include energy dissipation and is assumed to be given by

$$[C] = \mu[M] \tag{6}$$

where μ is a damping coefficient, $[K]$ is the linear stiffness matrix, and $[S]$ may be called a stability, loading or geometric stiffness matrix. Equation (5) is a set of Hill's equations or, if $[C] = 0$, a set of coupled Mathieu equations.

3. SOLUTION PROCEDURE

It is desired to determine boundaries of instability regions in the (ω, N) plane, based on the linear eqns (5). In order to simplify the computations involved in the stability analysis, the equations are first transformed such that $[M]$ and $[K]$ become diagonal matrices.

Since $[M]$ and $[K]$ are real, symmetric matrices and [M] is positive definite, there exists a real matrix $[P]$ such that (see Franklin, 1968)

$$[P]^T[M][P] = [I], \quad [P]^T[K][P] = [\Lambda] \tag{7}$$

where $[I]$ is the identity matrix, $[\Lambda]$ is a diagonal matrix, and $[\ ]^T$ denotes transpose of the enclosed matrix. If $\{\delta\}$ and $[R]$ are defined by

$$\{\Delta\} = [P]\{\delta\}, \quad [R] = [P]^T[S][P], \tag{8}$$

and (5) is pre-multiplied by $[P]^T$, one obtains

$$\{\ddot{\delta}\} + \mu\{\dot{\delta}\} + [\Lambda]\{\delta\} + N\cos\omega t[R]\{\delta\} = 0. \tag{9}$$

Some of the equations in (9) may be uncoupled (i.e. only involve a single component δ_i), and the rest may be separated into sets of equations which are uncoupled from each other. In other words, the equations in (9) can be rearranged so that $[R]$ becomes a block diagonal matrix. These single equations and sets of equations can be analyzed separately.

Let ω_i denote the natural frequencies of the undamped, unloaded system ($\mu = 0$, $N = 0$), with $\omega_1 \leqslant \omega_2 \leqslant \cdots$. The diagonal elements of Λ are squares of these natural frequencies. Attention is usually focused on resonances involving the lowest frequency ω_1, and the corresponding instability regions are then obtained using the set of equations which contains ω_1^2 as an element of $[\Lambda]$.

Bolotin's method is applied to the set of equations from (9) which is of interest (Bolotin, 1964). Let r be the number of those equations and $\{\eta\}$ the $r \times 1$ vector of the corresponding components of $\{\delta\}$. To obtain points on the boundaries of the instability regions, the components of $\{\eta\}$ are written in the Fourier series (Srinavasan and Chellapandi, 1986; Başar *et al.*, 1987):

$$\eta_i = \sum_{j=1}^{\infty} \left[a_{ji} \sin \frac{(2j-1)\omega t}{2} + b_{ji} \cos \frac{(2j-1)\omega t}{2} \right] \tag{10}$$

with period $2T$, where $T = 2\pi/\omega$, or

$$\eta_i = \tfrac{1}{2} b_{0i} + \sum_{j=1}^{\infty} [a_{ji} \sin j\omega t + b_{ji} \cos j\omega t] \tag{11}$$

with period T. These expressions are substituted into the equations of motion for $\{\eta\}$ and the coefficients of each sine and cosine term are set equal to zero, as well as the sum of the constant terms. For nontrivial solutions, the infinite determinants of the coefficients of these groups of linear homogeneous equations are equal to zero.

Approximate solutions can be obtained by truncating the determinants. The smallest possible truncation will be called the "first approximation" and corresponds to $j = 1$ in (10) and (11). The next smallest truncation, called the "second approximation" here, includes the $j = 1$ and $j = 2$ terms in (10) and (11). Consider the first approximation. For no damping ($\mu = 0$), (10) leads to two $r \times r$ determinants, while (11) leads to an $r \times r$ determinant and a $2r \times 2r$ determinant (Başar *et al.*, 1987). These determinants are linear eigenvalue problems in ω^2. When $\mu \neq 0$, (10) and (11) lead to $2r \times 2r$ determinants which involve ω and ω^2; each can be transformed into a $4r \times 4r$ determinant which is a linear eigenvalue problem in ω. For the second approximation, the determinants are twice as large.

In some cases, the matrix equation of motion for $\{\eta\}$ is almost diagonal. In other words, for the set of r equations from (9) which is being analyzed, the off-diagonal terms from $[R]$ may be much smaller than the diagonal terms. Then an approximate solution can be obtained by neglecting the off-diagonal terms. If $\mu = 0$, this leads to a Mathieu equation which can be put into the form

$$\frac{d^2\eta_i}{d\tau^2} + p\eta_i + 16q\eta_i \cos 2\tau = 0. \tag{12}$$

For sufficiently small values of q, the boundaries of the principal instability region can be determined approximately from (see Hayashi, 1985):

$$p = 1 \pm 8q - 8q^2 \pm 8q^3 - (8/3)q^4. \tag{13}$$

This procedure will be referred to as the "analytical approximation".

Results from the first, second, and analytical approximations will be compared. In addition, the equations of motion for $\{\eta\}$ will be integrated numerically to ascertain which of the approximate methods give an accurate prediction of the transition from stability to instability.

4. RESULTS

A "standard case" is defined, in which the plate is a square, four-layer, symmetric cross-ply laminate, 0°/90°/90°/0°, with equal-thickness plies (the lamination angle is measured with respect to the x axis). The edges of the plate are simply supported with no tangential in-plane displacements. The plate parameters in this standard case are

$$\begin{gathered} a = 10 \text{ in.}, \quad a/h = 25, \quad \rho = 1 \text{ lb in.}^{-3}, \quad \mu = 0, \\ k_4^2 = k_5^2 = 5/6, \quad E_2 = 10^6 \text{ psi}, \quad E_1/E_2 = 40, \\ G_{12}/E_2 = 0.6, \quad G_{23}/E_2 = 0.5, \quad \nu_{12} = 0.25, \\ G_{13} = G_{12}, \quad \nu_{13} = \nu_{12}, \end{gathered} \tag{14}$$

where E_1 and E_2 are layer elastic moduli in directions along the fibers and normal to them, respectively, G_{12} and G_{13} are layer in-plane shear moduli, G_{23} is the thickness shear modulus, and ν_{12} and ν_{13} are Poisson's ratios (Reddy, 1984; Jones, 1975).

In the standard case, results are obtained using the first approximation in Bolotin's method. The plate is divided into 64 square elements (i.e. an 8×8 mesh of bilinear elements), with five degrees of freedom per node. After the boundary conditions are applied, the vector $\{\Delta\}$ in (5) has 301 elements. The transformed system of equations, (9), separates into 154 uncoupled equations and 49 uncoupled sets containing three equations each. Unless otherwise stated, the results discussed here are associated with the standard case.

For this case, the equation containing the lowest natural frequency, ω_1, is coupled with equations involving ω_{151} and ω_{162}. The second and fourth frequencies, ω_2 and ω_4, are each also in a set of three equations. However, ω_3 only appears in a single equation, and the load is not present in that equation [i.e. the associated row of $[R]$ in (9) only has zero elements]. Hence, ω_3 is not involved in any resonance.

Instability regions are plotted in the plane having load frequency ω as abscissa and load amplitude N as ordinate. When damping is neglected, these regions are wedge-shaped with vertices on the abscissa at $\omega = 2\omega_j/m$ (resonance of the mth order) and at $\omega = (\omega_j \pm \omega_i)/m$ (combination resonances), where $m = 1, 2, \ldots$ (Bolotin, 1964; Evan-Iwanowski, 1976; Nayfeh and Mook, 1979). The regions with vertices at $\omega = 2\omega_j$ are called the principal instability regions.

Let

$$\bar{\omega} = \omega/\omega_1^s, \quad \bar{N} = N/N_{cr}^s \tag{15}$$

where ω_1^s is the lowest natural frequency for the standard case and N_{cr}^s is the static critical

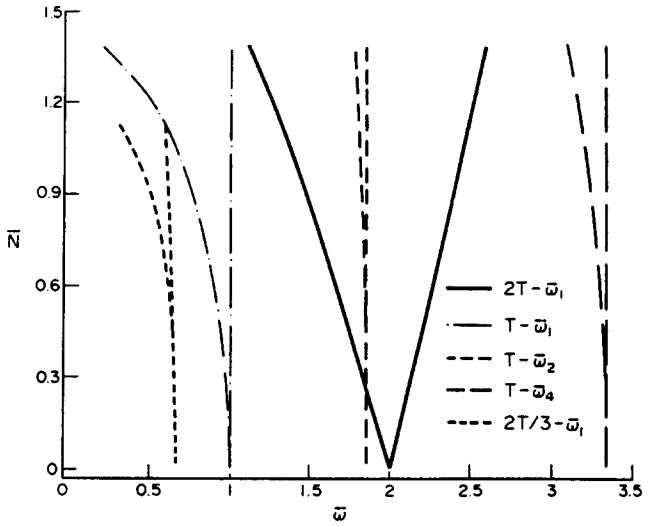

Fig. 2. Instability regions for standard case (four layers, 0°/90°/90°/0°).

load for that case. Figures 2–7 are in terms of these nondimensional quantities. Some instability regions in the range $0 \leqslant \bar{\omega} \leqslant 3.5$ are depicted in Fig. 2. The region denoted $2T-\bar{\omega}_1$ refers to the principal instability region associated with ω_1 and has its vertex at $\omega = 2\omega_1$. The region marked $T-\bar{\omega}_1$ has its vertex at $\omega = \omega_1$ and is called an instability region of second order. Other second-order regions in Fig. 2 are the narrow central region, $T-\bar{\omega}_2$, with its vertex at $\omega = \omega_2$, and the right-most region, $T-\bar{\omega}_4$, with its vertex at $\omega = \omega_4$. The left-most region, $2T/3-\bar{\omega}_1$, which was obtained using the second approximation in Bolotin's method, is a third-order region with its vertex at $\omega = 2\omega_1/3$. Other regions in the range of Fig. 2 are very narrow and are not depicted.

As the load amplitude $\bar{N}$ increases, the instability regions begin to overlap. When N is equal to the static critical load (i.e. $\bar{N} = 1$), the plate is unstable for about half the range of load frequencies shown in Fig. 2. If $\bar{N}$ is sufficiently large, the plate will be unstable for any load frequency.

The principal instability region is by far the largest one in Fig. 2. It becomes even more significant relative to the other regions when damping is taken into account. In the

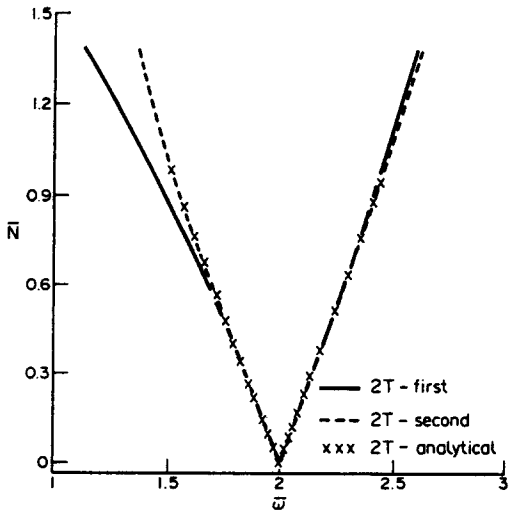

Fig. 3. Principal instability region for standard case determined by different solution procedures.

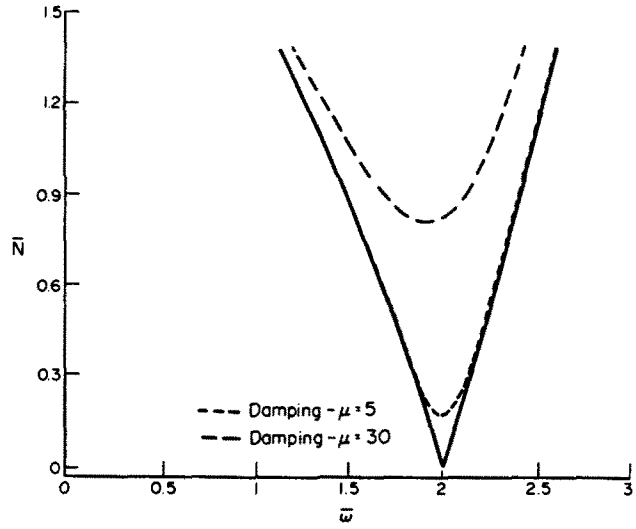

Fig. 4. Effect of damping on principal instability region for standard case.

subsequent figures, which illustrate the effects of the solution procedure and various properties of the plate, only the principal instability region associated with the lowest natural frequency will be plotted.

Results based on different solution procedures are depicted in Fig. 3. Solid curves give the instability region boundaries based on the first approximation, dashed curves are computed from the second approximation, and the crosses are obtained from the analytical approximation. In the submatrix of $[R]$ included in the three equations containing the first mode, the largest off-diagonal term R_{ij} is less than 4% of the smallest diagonal term R_{ii} (in magnitude), so that the governing set of equations is nearly diagonal.

For certain combinations of $\bar{\omega}$ and $\bar{N}$ near the instability boundaries, the set of three equations was integrated numerically, and the resulting transition points from stability to instability were found to be almost identical with points on the boundaries based on the second approximation. Since the analytical and second approximations yield similar results in Fig. 3, the numerical integration results imply that both are very accurate in this case. The first approximation also furnishes accurate results if the load amplitude is sufficiently small.

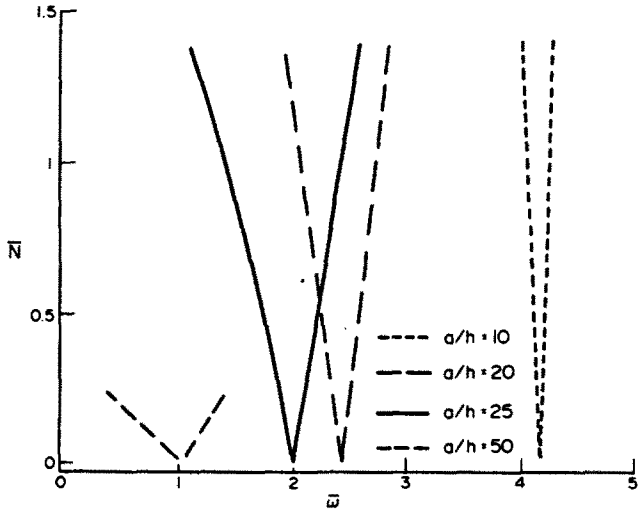

Fig. 5. Effect of ratio of edge length to thickness on principal instability region for standard case.

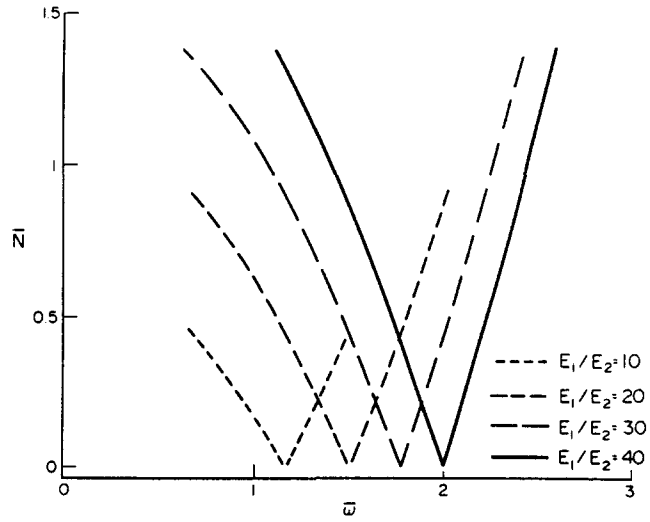

Fig. 6. Effect of orthotropy on principal instability region for standard case.

Figure 4 illustrates the effect of damping on the principal instability region. The wedge-shaped region for $\mu = 0$ becomes smaller as μ is increased. For other regions, the minimum value of $\bar{N}$ for instability is substantially higher than for the principal region. If the damping matrix $[C]$ were not proportional to the mass matrix $[M]$, it is possible that the damped regions would be wider than the undamped region above some value of $\bar{N}$, causing some stable combinations of $\bar{\omega}$ and $\bar{N}$ to become unstable as damping is increased (Nayfeh and Mook, 1979).

Four different ratios of the plate edge length, a, to the plate thickness, h, are considered in Fig. 5. Since $\bar{\omega}$ and $\bar{N}$ are nondimensionalized with respect to ω_1 and N_{cr} for the standard case $a/h = 25$ (solid curves), the vertices do not coincide (at $\bar{N} = 0$) and $\bar{N}$ is not equal to unity at the static critical load for the other cases. At a given value of load amplitude N, as the ratio a/h increases, the load frequencies ω for which principal parametric instability occurs tend to decrease and their range (i.e. the width of the instability region) increases. This result cannot be directly compared with that of Bert and Birman (1987) due to differences in nondimensionalization.

The influence of the ratio E_1/E_2 is demonstrated in Fig. 6, with $E_1/E_2 = 40$ for the standard case. If N is fixed and the ratio E_1/E_2 is decreased, the values of ω for instability tend to decrease and the range of values increases.

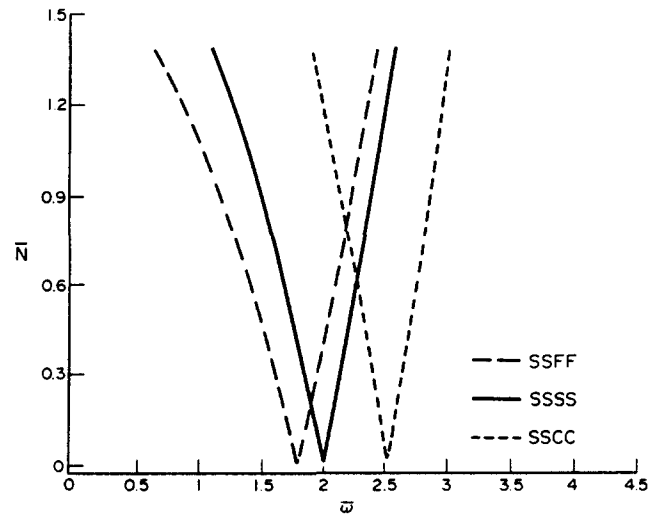

Fig. 7. Effect of boundary conditions on principal instability region for standard case.

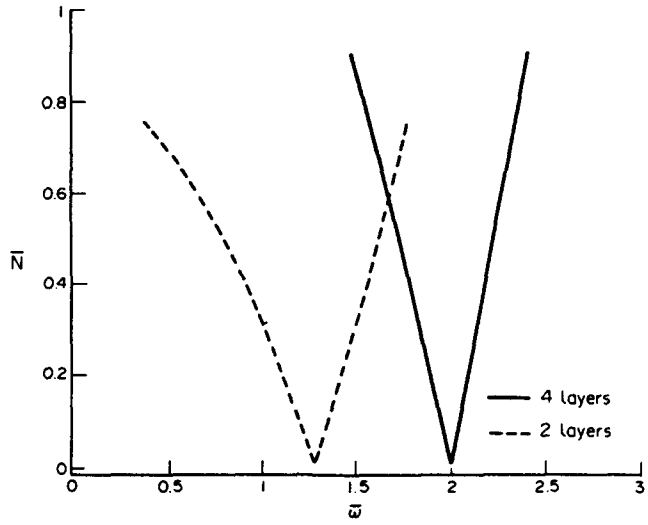

Fig. 8. Effect of number of layers on principal instability region for antisymmetric angle-ply laminate (two layers: 45°/−45°; four layers: 45°/−45°/45°/−45°).

Results for three sets of boundary conditions are presented in Fig. 7, where SSSS refers to the standard case, with all edges simply supported. For SSFF, the load acts along simply supported parallel edges and the other two parallel edges are free. The principal instability region shifts to lower frequencies and is slightly wider than that for the standard case at a given value of N. For SSCC, the loaded edges are again simply supported and the other two edges are clamped. In this case the region shifts to higher frequencies and becomes slightly more narrow.

Figures 8 and 9 deal with antisymmetric angle-ply laminates. The other difference from the standard case is that normal (rather than transverse) in-plane displacements are prevented at the edges. The transformed equations of motion, (9), can be separated into 70 uncoupled equations, seven sets with three equations each, and 21 sets with 10 equations each. The equation containing ω_1 is coupled with equations involving ω_{59} and ω_{130}.

Figure 8 illustrates the effect of different numbers of layers. The lamination scheme is 45°/−45° for the two-layer plate and 45°/−45°/45°/−45° for the four-layer plate. Both have $a/h = 25$, and nondimensionalization along the axes is relative to ω_1 and N_{cr} of the

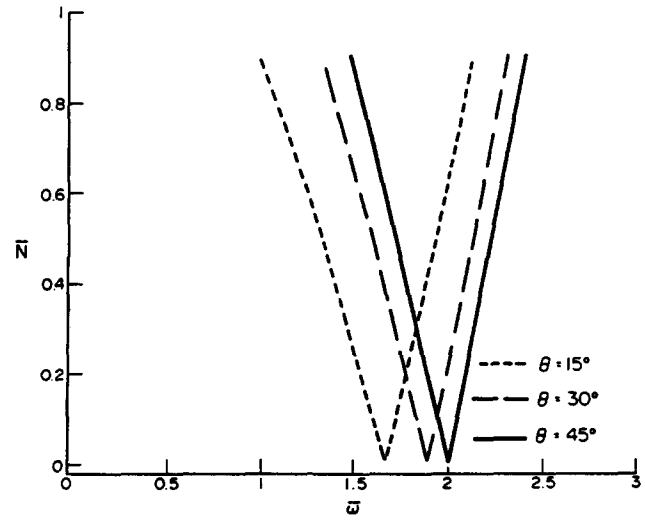

Fig. 9. Effect of lamination angle on principal instability region for four-layer antisymmetric angle-ply laminate ($\theta/-\theta/\theta/-\theta$).

four-layer plate, respectively. The instability region has lower frequencies and is wider for the two-layer case. A similar shift to lower frequencies was found in Bert and Birman (1987).

Several lamination angles are considered in Fig. 9. The case $\theta = 45^\circ$ is the same as the four-layer plate treated in Fig. 8, and $\bar{N}$ and $\bar{\omega}$ are defined in the same way. In the other cases, also with four layers, the alternating angles of the fibers with the x axis are $\theta = 30^\circ$ and $\theta = 15^\circ$, respectively. As the angle θ decreases in magnitude, the principal instability region shifts to lower frequencies and widens.

5. CONCLUDING REMARKS

The finite element method with the first-order shear deformation laminate plate theory was applied to investigate parametric instability of composite laminates subjected to harmonically-varying in-plane loads. Transverse shear deformation was taken into account. When the linear equations of motion were transformed, the mass matrix and elastic stiffness matrix became diagonal and the stability (loading) matrix took a block diagonal form. Only sets of a small number of coupled equations had to be analyzed to obtain boundaries of instability regions.

In some cases, the set of equations of interest was nearly diagonal, and approximate results could be obtained neglecting the off-diagonal terms. Otherwise, Bolotin's method was used, with two sizes of subdeterminants examined (first and second approximation). In the standard case treated here, there were 301 generalized displacements. Corresponding to each of the 301 frequencies of vibration is a principal instability region and an infinite number of other instability regions. There are also instability regions associated with combinations of frequencies. As is typical, attention was primarily focused on the principal instability region corresponding to the lowest natural frequency.

The plate was square and the loading was uniaxial with no static component, but these assumptions could be relaxed without any difficulty. Symmetric cross-ply laminates and antisymmetric angle-ply laminates were treated. Various effects were analyzed: solution procedures, damping, ratio of edge length to thickness of the plate (a/h), orthotropy (E_1/E_2), boundary conditions, number of layers, and lamination angle (θ). The locations and widths of the instability regions varied in the (ω, N) plane. In the numerical results, the principal instability region associated with the lowest natural frequency tended to shift to lower frequencies and to widen as the edges became less constrained, a/h increased, or E_1/E_2, θ, or the number of layers decreased.

Acknowledgements—This research was supported in part by the U.S. Army Research Office under Grant No. DAAL03-87-K-0040. The authors are grateful to Professor V. Birman for supplying them with copies of his related papers.

REFERENCES

Başar, Y., Eller, C. and Krätzig, W. B. (1987). Finite element procedures for parametric resonance phenomena of arbitrary elastic shell structures. *Computational Mech.* **2**, 89–98.

Bert, C. W. and Birman, V. (1987). Dynamic instability of shear deformable antisymmetric angle-play plates. *Int. J. Solids Structures* **23**, 1053–1061.

Bert, C. W. and Birman, V. (1988). Parametric instability of thick, orthotropic, circular cylindrical shells. *Acta Mech.* **71**, 61–76.

Birman, V. (1985). Dynamic stability of unsymmetrically laminated rectangular plates. *Mech. Res. Commun.* **12**, 81–86.

Birman, V. (1989). Problems of dynamic buckling of antisymmetric rectangular laminates. *Composite Struct.* **12**, 1–15.

Birman, V. and Bert, C. W. (1988). Nonlinear parametric instability of antisymmetrically laminated angle-ply plates. *Dynamic Stability Systs* **3**, 57–68.

Birman, V. and Zahed, H. (1989). Nonlinear problems of parametric vibrations of imperfect laminated plates. *Composite Struct.* **12**, 181–191.

Bolotin, V. V. (1964). *Dynamic Stability of Elastic Systems*. Holden-Day, San Francisco.

Evan-Iwanowski, R. M. (1976). *Resonance Oscillations in Mechanical Systems*. Elsevier, New York.

Franklin, J. (1968). *Matrix Theory*. Prentice-Hall, New York.

Hayashi, C. (1985). *Nonlinear Oscillations in Physical Systems*. Princeton University Press, Princeton.

Hildebrand, F. B., Thomas, G. B. and Reissner, E. (1949). Note on the foundations of the theory of small displacements of orthotropic shells. NACA TN-1833, Washington, D.C.

Jones, R. M. (1975). *Mechanics of Composite Materials*. Hemisphere, New York.

Mindlin, R. D. (1951). Influence of rotatory inertia and transverse shear deformation on the flexural motion of isotropic, elastic plates. *J. Appl. Mech.* **12**, 31–38.

Nayfeh, A. H. and Mook, D. T. (1979). *Nonlinear Oscillations*. Wiley-Interscience, New York.

Noor, A. K. and Burton, W. S. (1989). Assessment of shear deformation theories for multilayered composite plates. *Appl. Mech. Rev.* **42**, 1–12.

Reddy, J. N. (1984). *Energy and Variational Methods in Applied Mechanics*. John Wiley, New York.

Srinivasan, R. S. and Chellapandi, P. (1986). Dynamic stability of rectangular laminated composite plates. *Comput. Struct.* **24**, 233–238.

Tylikowski, A. (1989). Dynamic stability of nonlinear antisymmetrically-laminated cross-ply rectangular plates. *J. Appl. Mech.* **56**, 375–381.